Herpesvirus saimiri-based endothelin-converting enzyme-1 shRNA expression decreases prostate cancer cell invasion and migration

ARTICLE *in* INTERNATIONAL JOURNAL OF CANCER · AUGUST 2011

Impact Factor: 5.09 · DOI: 10.1002/ijc.25719 · Source: PubMed

6 AUTHORS, INCLUDING:

Yue Hong
The Jackson Laboratory
8 PUBLICATIONS **23** CITATIONS

uicc
global cancer control

IJC
International Journal of Cancer

Herpesvirus saimiri-based endothelin-converting enzyme-1 shRNA expression decreases prostate cancer cell invasion and migration

Yue Hong[1], Stuart Macnab[1], Louise A. Lambert[1], Anthony J. Turner[1], Adrian Whitehouse[1,2] and Badar A. Usmani[1]

[1] Institute of Molecular and Cellular Biology, Faculty of Biological Sciences, University of Leeds, Leeds, United Kingdom
[2] Astbury Centre for Structural Molecular Biology, University of Leeds, Leeds, United Kingdom

The zinc metalloprotease, endothelin-converting enzyme-1 (ECE-1), which converts the mitogenic peptide endothelin-1 (ET-1) from its biologically inactive precursor big-ET-1, is commonly upregulated in prostate cancer (PC) cells. Consequently, we have sought to suppress ECE-1 expression by using RNAi as a potentially novel therapeutic approach. Therefore, a synthetic 64-nt short-hairpin RNA (shRNA), designed to target the ECE-1 gene, was expressed in an Herpesvirus saimiri (HVS)-based delivery vector. ECE-1 expression in cells transduced with the vector was examined by real-time PCR and Western blotting. The effects of ECE-1 knockdown on PC cell migration and invasion were studied using a scratch assay and Matrigel invasion. These studies, *in vitro* and *ex vivo*, demonstrated that the HVS-shRNA viruses could infect and silence ECE-1 expression effectively in human PC cells. Furthermore, it was observed that ECE-1 knockdown in either stromal cells or epithelial cells could significantly reduce invasion of PC-3 cells in coculture by 33 and 31%, respectively. In addition, suppressed migration was also observed in HVS-ECE-1 shRNA-infected PC-3 cells compared to uninfected and HVS-GFP-infected control cell cultures. These findings highlight the potential tumor-suppressing effect of ECE-1 knockdown in cancer cells and novel strategies for future therapeutic developments in advanced PC.

Prostate cancer (PC) is the most frequently diagnosed cancer and the second leading cause of cancer death in western males.[1] Although androgen withdrawal can initially give effective control of cancer progression,[2] subsequent transition to the more malignant and metastatic androgen-independent form, which is neuropeptide-driven, requires novel approaches to treatment. In particular, the upregulation of protein components involved in the endothelin-1 (ET-1) signaling axis plays a key role in progression of many types of cancer, including ovarian, colorectal, breast and PC.[3–6] Specifically, plasma levels of ET-1 are abnormally elevated in patients with advanced, androgen-independent PC[7], and the potent ET receptor subtype A (ET_AR) antagonist atrasentan (ABT-627) has been reported to suppress partially prostate tumor growth.[8] Hence, inhibition of ET formation or downstream signaling could provide a novel strategy to treat advanced PC.

Key words: prostate cancer, endothelin, endothelin-converting enzyme-1, Herpesvirus saimiri, metalloprotease, neprilysin
Grant sponsors: Yorkshire Cancer Research, Prostate Cancer Research Foundation and Prostate UK
DOI: 10.1002/ijc.25719
History: Received 18 May 2010; Accepted 9 Sep 2010; Online 14 Oct 2010
Correspondence to: Anthony J. Turner, Institute of Molecular and Cellular Biology, Faculty of Biological Sciences, University of Leeds, Leeds LS2 9JT, United Kingdom, Tel.: +44-113-343-3131, Fax: +44-113-343-3157, E-mail: a.j.turner@leeds.ac.uk

The final and rate-limiting step in the biosynthesis of ET-1 is catalyzed by endothelin-converting enzyme-1 (ECE-1), a 120–130 kDa integral membrane-associated glycoprotein, belonging to the M13 zinc-metalloprotease family, which also includes neprilysin (NEP), the major ET-1 degradative enzyme.[9] Four isoforms of ECE-1 (ECE-1a–1d) have been identified, which are transcribed from a single gene using alternative promoters.[10,11] They have a common catalytic domain but show distinct subcellular localization because of the differences in their N-terminal tails, with ECE-1a and ECE-1c predominantly being expressed at the plasma membrane, whereas ECE-1b and ECE-1d mainly occur in endosomal membranes.[10,12] Although cell surface ECE-1 is known to be responsible for the activation of big ET-1 and inactivation of bradykinin,[13,14] endosomal ECE-1, which can degrade various peptides such as substance P (SP) and calcitonin gene-related peptide (CGRP),[15] has been suggested to play an important role in the recycling and desensitization of internalized receptors.[16] NEP and ECE-1 appear to be reciprocally regulated in a number of cancers with ECE-1 levels frequently elevated.[5,17,18] Although all ECE-1 isoforms show transcription in the human prostate cell lines and primary stromal cells, only ECE-1c produces significant amounts of ECE-1 protein in prostate cell lines. In addition, only ECE-1b and 1c proteins were detected in primary stromal cells, with increased levels in the malignant state when compared to benign.[19] Furthermore, ECE-1c is also reported by Ahmed *et al.*[20] as the most abundant isoform in lung cancer cells. Hence, suppressing the production of ECE-1 is thought to be

a therapeutic option in PC and other cancers. In this context, we have previously reported that using siRNA, which targeted a common sequence of all ECE-1 isoforms, could effectively block proliferation of oral squamous carcinoma cells.[21] However, the siRNA oligonucleotides only provide a transient effect in transfected cells, and cellular uptake is generally limited in *ex vivo* and *in vivo* environments.

To overcome these problems, we have exploited a viral vector to facilitate ECE-1 siRNA transfer and expression in PC cells and examined the effects on invasivity. Although adenoviral, retroviral and adeno-associated viral short-hairpin RNA (shRNA) delivery systems have been successfully exploited to silence genes *in vitro* and *in vivo*,[22–25] they possess a major drawback either in strong immunogenicity or in unexpected endogenous oncogene expression because of the potential integration of viral DNA into the host genome.[26–28] As a consequence, we have used Herpesvirus saimiri (HVS), a dsDNA γ-2 herpesvirus, as the gene therapy vector, which is maintained in infected cells as a nonintegrated circular episome. The ability of HVS to be maintained extrachromosomally avoids the occurrence of insertional mutagenesis and rapid silencing of heterologous transgene expression caused by chromosome integration.[29] An additional advantage of this delivery vector in cancer gene therapy is its ability to infect a variety of human carcinoma cell lines at approaching 100% efficiency.[30,31] Furthermore, upon infection of human cells, it can exist in a latent, asymptomatic state reducing immune system clearance. These attributes therefore support the use of an HVS-based vector as a potent, safe and efficient delivery vehicle in gene therapy research.

In our study, we have constructed an HVS-based vector expressing an ECE-1-targeted shRNA to stably suppress ECE-1 expression in PC. We have tested the feasibility of delivery of HVS-shRNA in various PC cell lines and primary cells and, for the first time, demonstrated the potential influence of ECE-1 knockdown by RNAi on PC cell invasion and migration.

Material and Methods

Cell culture

PC-3 cells were maintained in Ham's F-12 supplemented with 7% fetal bovine serum (FBS) and 2 mM L-glutamine. The mouse embryonic fibroblast cell line, STO, and owl monkey kidney (packaging) cell line, OMK, were maintained in DMEM medium containing 10% FBS and 2 mM L-glutamine. The colorectal carcinoma cell line, SW480, was grown in RPMI 1640 containing 10% FBS and 2 mM L-glutamine. Primary prostate stromal cells isolated from a Gleason grade 7 prostatectomy (herein referred to as G7), and the PNT2-C2 cell line (normal transformed prostate cells with low invasive ability), were kindly provided by Prof. N. Maitland (York Cancer Research Unit, York, UK). Both cell lines were routinely cultured in RPMI 1640 containing 10% FBS and 2 mM L-glutamine. All culture reagents were purchased from Biowhittaker, Wokingham, UK. All cells were maintained at 37°C in a humidified atmosphere containing 5% CO_2.

Stage 1: Construction of a pSUPER shRNA vector

A 19-nt ECE-1-targeting siRNA was designed as follows: 5′-CUUCCACAGCCCCCGGAGUdTdT-3′ (sense) and 5′-ACUCCGGGGGCUGUGGAAGdTdT-3′ (antisense) recognizing the ECE-1 gene 142–162 nt downstream of the start codon. A 64-nt shRNA against the ECE-1 transcript was constructed based on the 19-nt siRNA sequence (see Fig. 1*a*). The forward and reverse oligonucleotides were annealed, and the resulting dsDNA was ligated into the *BglII-HindIII* sites of the pSUPER vector (Fig. 1*b*), immediately downstream of a RNA polymerase III-dependent H1 promoter. Ligation was carried out at room temperature for 2 hr using T4 ligase (New England Biolabs, Herts, UK). Constructed vectors were transformed into DH5α cells and positively selected on LB agar containing 50 μg/ml ampicillin. shRNA insertion was confirmed by 2% agarose gel electrophoresis and DNA sequencing (Lark Technologies, Essex, UK).

Stage 2: Construction of a pShuttle-Link1 shRNA shuttle vector

The ECE-1-targeting shRNA fragment with H1 promoter sequence was excised from pSUPER-shRNA and cloned into pShuttle-link1 vector between the *XbaI-SnaBI* sites (Fig. 1*c*). Ligation was identical to Stage 1. Selection was performed with 50 μg/ml kanamycin.

Stage 3: Construction and purification of an infective HVS-BAC-shRNA vector

Following *I-Ppo I* (Promega, Madison, WI) digestion, the enzyme was heat inactivated, and salts were excluded from the linearized HVS-GFP-BAC (Fig. 1*d*) by drop dialysis using a 0.025-μm nitrocellulose membrane filter (Millipore, Watford, UK). The shRNA cassette was excised from the pShuttle vector and purified by gel extraction as per the manufacturer's instructions (Invitrogen, Paisley, UK). Ligation reactions were carried out at 16°C overnight. Recombinant HVS-BAC-shRNA was transformed into DH10β cells by electroporation and selected against 50 μg/ml kanamycin and 12.5 μg/ml chloramphenicol. shRNA insertion was checked by pulse-field electrophoresis (10 hr, 6 V/cm, ramped switch time 2–16 sec, using a Bio-Rad PFG system; Bio-Rad Laboratories, Hemel Hempstead, UK) on a 1.2% agarose gel. Virus packaging was performed in an OMK permissive cell line. HVS-BAC-shRNA was transfected into OMK cells by Lipofectamine 2000 (Invitrogen) as per the manufacturer's instructions. After overnight transfection at 37°C, transfection medium was replaced with fresh culture medium for the remaining period of virus production. When cell lysis was complete, 2 ml aliquots of supernatant containing infective particles was used in second-round infections of OMK cells to amplify virus.

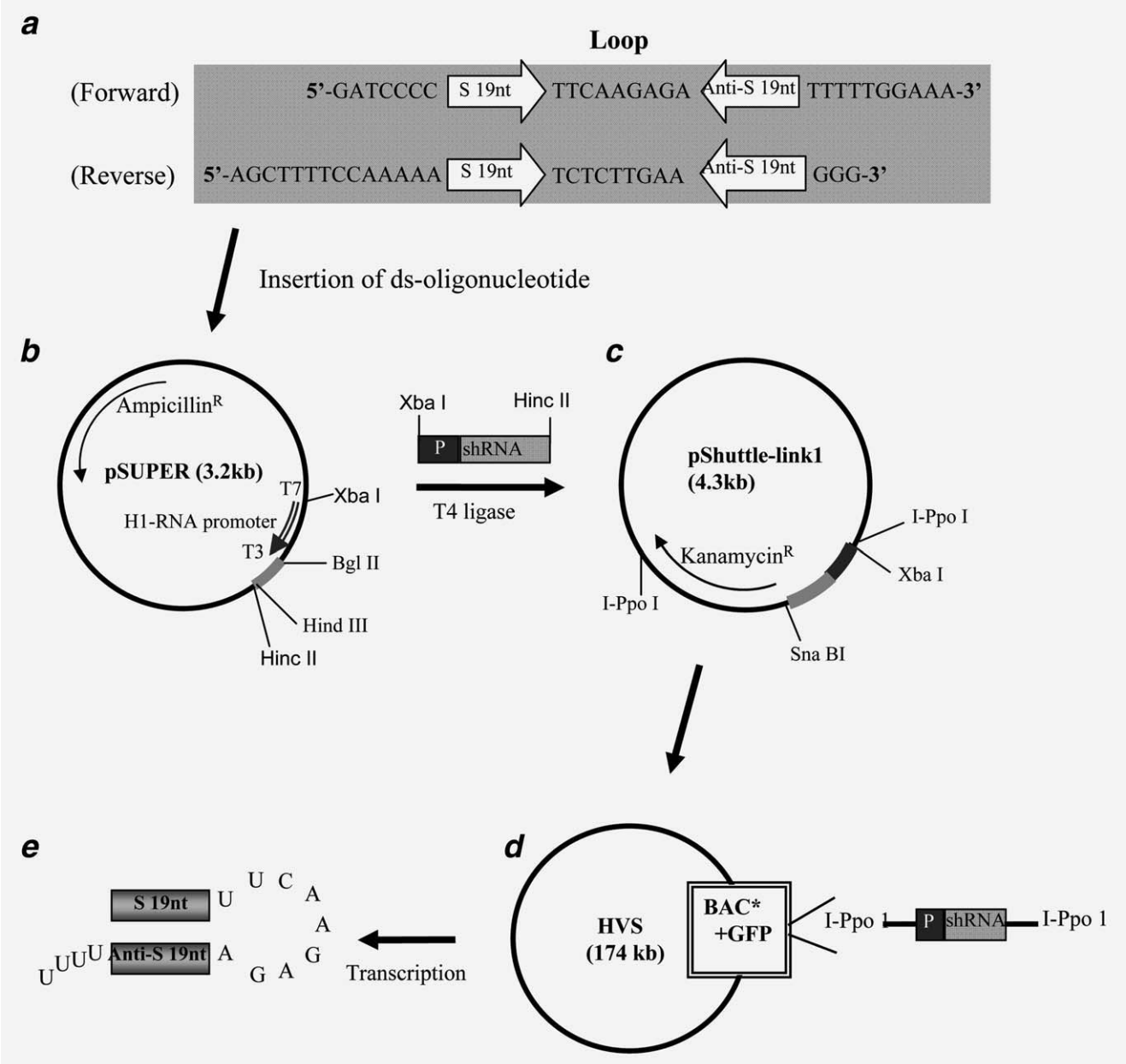

Figure 1. Flowchart showing the three-stage construction of an HVS-BAC-shRNA vector. (*a*) A 64-nt oligonucleotide was constructed of a sense (S 19 nt) and an antisense (anti-S 19 nt) sequence of ECE-1-targeting siRNA with an additive loop. (*b–d*) Schematic drawing of three vectors involved in the construction process. *HVS-bacterial artificial chromosome (HVS-BAC), which contains selectable markers Chloramphenicol^R and Hygromycin^R. This BAC cassette enables the viral genome to be maintained in *E. coli* and modified by routine cloning methods. (*e*) Short-hairpin RNA (shRNA) was transcribed by vectors under the control of the RNA polymerase III-dependent H1 promoter to produce functional siRNA after Dicer cleavage.

Virus titration

OMK cells were preseeded in six-well plates and allowed to achieve 90% confluency. Fifty microliters of HVS-GFP-shRNA was used to infect each well. After 48-hr incubation, cells were harvested, resuspended in phosphate-buffered saline (PBS) and GFP-positive cells counted using a Becton Dickson FACScalibur flow cytometer. Virus concentrations as plaque-forming units per milliliter (PFU/ml) were determined as a mean of three independent infections.

Transfection

Cells were routinely seeded at 60% confluency 24 hr before transfection. PC-3 cells were transfected using a prostate cell-specific transfection kit (Mirus Bio LLC, Madison, WI), and

STO cells were transfected using Fugene 6 (Roche Diagnostics, Burgess Hill, UK) according to the manufacturer's guidelines. To estimate transfection efficiency, an equivalent amount of GFP control vectors were transfected into a separate flask under the same conditions, and GFP-positive cells were monitored by fluorescence microscopy.

Transduction

Target cells were seeded at >80% confluency in either six-well plates or tissue culture flasks 24 hr before transduction. The following day, virus was added directly onto fresh media overlaying cells at a multiplicity of infection (MOI) of ~1–2. Culture medium was replaced every 48 hr to remove dead cells and debris. Stably infected cells identified by GFP expression provided an indication of infection efficiency.

Western blotting

Cellular proteins (30 μg) were separated on 3–8% Tris-acetate SDS-PAGE precast gels (Invitrogen), transferred to a nitrocellulose membrane (Invitrogen) and blocked in TBST (10 mM Tris-Cl, pH 7.4 with 0.05% Tween-20) containing 5% (w/v) milk powder. Membranes were incubated with the following antibodies: anti-ECE-1 monoclonal antibody, AEC 32-236 (generously donated by Dr. K. Tanzawa, Sankyo Research Laboratories, Tokyo; 1:200), anti-ECE-1 polyclonal antibody[32] (1:200) and anti-β-actin antibody (Sigma-Aldrich, Gillingham, Dorset, UK; 1:10,000). After incubation with anti-mouse or anti-rabbit horseradish peroxidase-conjugated secondary antibodies (Novagen, Merck Chemicals, Nottingham, UK; 1:2,000), specific protein bands were visualized using enhanced chemiluminescence (Pierce ECL, Thermo Fisher Scientific, Northumberland, UK) according to the manufacturer's instructions.

Immunofluorescence

PC-3 cells were grown on sterile cover slips in six-well culture plates at 60% confluency 24 hr before transfection. At 72 hr post-transfection, cells were fixed in 3.7% formaldehyde (Sigma, UK) for 5 min, permeabilized using 0.1% Triton X-100 in PBS for 5 min and then fixed again for 5 min at room temperature. Any residual formaldehyde was quenched using NH_4Cl for 10 min. Nonspecific binding sites were blocked with 5% (v/v) normal goat serum for 30 min. Cells were labeled with anti-ECE-1 antibody (1:20 in blocking buffer) for 2 hr, washed with PBS and then incubated with Alexa Fluor Molecular Probe 594 goat anti-mouse secondary antibody (Invitrogen; 1:1,000 in blocking buffer) for 30 min. After counterstaining with 4′,6-diamidino-2-phenylindole (DAPI; 1:1,000 in PBS), cells were washed with PBS and mounted on glass slides using Vectashield (Vector Laboratories, USA). Cells were viewed and photographed using an inverted wide-field fluorescence microscope.

Real-time PCR

RNA was extracted from transduced cells using a Qiagen RNeasy RNA preparation kit. Purity and concentration of preparations were measured by UV spectrophotometry. cDNA synthesis was performed using an iScript cDNA synthesis kit (Bio-Rad) according to the manufacturer's instructions. Standard samples consisted of serial dilutions of pCDNA3.1-hECE-1c, as described by Hunter and coworkers[21] (~0.01–100 pg). GAPDH was used as a reference gene. The reaction protocol was as follows: 10 ng of cDNA, 500 nM ECE-1 forward primer: 5′-GGACTTCTTCAGCTACGCCTGT-3′, 500 nM reverse primer: 5′-CTAGTTTCGTTCATACACGCACG-3′ and 1× iQ SYBR Green Supermix (Bio-Rad). The reaction mix was subjected to the following amplification cycle: 3 min at 95°C; 35 cycles at 95°C, 30 sec; 57°C, 30 sec; 72°C, 30 sec in a iCycler thermal cycler (Bio-Rad). Fluorescence was recorded by an iCycler iQ Real-Time Detection System.

Invasion assay

Invasion chambers were prepared using Matrigel (Becton Dickinson U.K.; 250 μg/ml), which was layered (200 μl) onto each cell culture insert (8 μm pore) and incubated overnight at 37°C. In parallel, primary prostate stromal cells (G7) were seeded into 24-well insert companion plates at 100% confluency and incubated overnight at 37°C. The following day, spent culture medium was removed from the stromal cells and replaced with 0.5 ml assay medium (DMEM containing 0.1% (w/v) BSA). Next, the Matrigel-containing inserts were placed into the wells of the companion plates, and 250 μl of an 8×10^5 cells per milliliter prostate epithelial cell suspension in assay medium was layered onto the Matrigel. When an ET-1 supplement was applied, ET-1 at a final concentration of 10 and 100 nM was added to the assay medium in both insert and stromal culture. The invasion assay was incubated for 24 hr at 37°C. Cells were then washed in PBS, fixed in 100% methanol for 10 min and stained with 0.1% (w/v) Crystal Violet. PC-3 cells that had invaded through the underside of the inserts were counted by light microscopy. Four fields of view were counted from each insert. Results were presented as average number of cells per field ± SEM and tested for statistical significance.

Scratch assay

PC-3 cells were seeded in six-well plates (≥90%) 24 hr before infection and then infected by either HVS-GFP or HVS-shRNA as described above. After 72-hr infection, the cell monolayer was scraped in a straight line to create a "scratch" with a p1000 pipette tip. Cells were washed with PBS to remove any cell debris and smooth the edge of the scratch and then incubated in normal culture medium at 37°C for 24 hr, with or without additive ET-1. "Scratch" images were acquired at 0, 12 and 24 hr, respectively, under bright-field conditions. Infection efficiency was monitored by GFP expression using fluorescence microscopy.

ELISA

ET-1 secretion was measured by an endothelin enzyme immunoassay kit (Cayman Chemical, Cambridge Bioscience, Cambridge, UK) following the manufacturer's instruction. PC-3 cells were infected as described above, and culture medium was replaced with serum-free Ham's F-12 8 hr before collection.

Statistical analysis

Densitometric analysis of Western blots was carried out by Image J, and quantitation of scratch assay was achieved by the S.CORE image analysis system. All results were expressed as the mean ± SD for three independent measurements unless otherwise stated in the figure legend. Significance of difference was assessed by two-tailed Student's *t*-test, and differences with $*p < 0.05$ and $**p < 0.001$ were considered to be statistically significant.

Results

Vector-mediated shRNA expression suppressed ECE-1 synthesis in ECE-1-expressing cell lines

A 64-nt double-stranded shRNA sequence was first cloned into pSUPER and then into pShuttle, during construction of the HVS-based shRNA expression vector (Fig. 1). Directional ligation was confirmed following each round of cloning. Efficacy of ECE-shRNA expression was then determined in PC-3 and STO cells, which express endogenous ECE-1.

To overcome inherent poor PC-3 transfection efficiency, a prostate-specific transfection kit (Mirus) was used. Immunofluorescence analysis revealed greatly reduced ECE-1 expression in PC-3 cells transfected with pSUPER-shRNA 72 hr post-transfection, compared to "empty" vector and untransfected controls (Fig. 2*a*). Similar results were obtained by Western analysis of pSUPER-shRNA-transfected PC-3 cells (Fig. 2*b*). A second transfection applied 24 hr after the first was aimed to improve transfection efficiency further on PC-3 cells. By densitometry, the "booster" transfection resulted in a 50% reduction in ECE-1 expression at 72 hr and 30% reduction at 96 hr (Fig. 2*c*).

As with pSUPER above, "booster" transfections were applied to pShuttle-shRNA transfections in PC-3 and STO cells. ECE-1 levels were reduced in both PC-3 and STO cells 72 hr post-transfection by 40 and 30%, respectively, when compared to its levels in untranfected controls (Fig. 2*d*). These data confirmed correct orientation and transcription of the shRNA fragment.

HVS-BAC-shRNA production using an OMK packaging cell line

To construct a viral vector capable of delivering the designed shRNA, the expression cassette located between the *I-Ppo I* sites on the pShuttle-link1 vector was excised, purified and ligated into the HVS bacterial artificial chromosome (BAC), which contains a unique *I-Ppo I* restriction site designed specifically for the rapid generation of viral vectors *via* modification of its large genome in *E. coli*.[33] Clones were analyzed *via* pulse-field gel electrophoresis (Fig. 3*a*). Clones (marked as * in the figure) were selected for the production of virus particles.

To generate and amplify HVS-BAC-shRNA infectious particles, the permissive cell line OMK was used (Fig. 3*b*). Further rounds of HVS-BAC-shRNA particles were amplified in OMK cells. Harvested and concentrated HVS-BAC-shRNA and WT-HVS-BAC stocks used in our experiments consistently had concentrations ranging from 7.8 to 8.4 $\times$ 10^6 PFU/ml.

HVS-BAC-shRNA virus shows good infection without cytotoxicity

The human colorectal carcinoma cell line, SW480, shows high infectivity with HVS and was used here as a positive control. Infection of SW480 cells with the WT-HVS-BAC and HVS-BAC-shRNA stocks was tested to establish the infection efficiency of the constructed viruses. As shown in Figure 4*a*, infection efficiency for both was comparable at 48–96 hr postinfection.

To test the effect of HVS-BAC-shRNA on human PC cells, PNT2C2, PC-3 and G7 cells were used, which represent the normal, malignant epithelial and malignant-derived stromal cells, respectively. After infection with HVS-BAC-shRNA at MOI = 2, GFP-positive cells could be detected in all cell types at 48 hr postinfection and reached very high percentages in both malignant PC-3 and G7 stroma ($\geq$80%) but much lower in PNT2C2 cells ($\leq$30%) even after 96 hr (Fig. 4*b*). To confirm that HVS had entered a latent state in human prostate cells, culture medium was collected from each group of transduced cells and overlain onto OMK cells. No GFP was detected after 48 hr incubation in OMK cells, which indicated that HVS-BAC-shRNA infection of the prostate cells did not induce cell lysis and virus release under these conditions (data not shown).

After an extended incubation time of up to 120 hr, expression of GFP protein could still be observed in transduced G7 cells, which provided direct evidence of sustained transgene expression. In addition, compared to the uninfected population, G7 cells transduced with either WT-HVS-BAC or HVS-BAC-shRNA did not show an obvious difference in cell morphology or growth rate until 120 hr postinfection (Fig. 4*c*).

HVS-BAC-shRNA virus reduced endogenous ECE-1 transcription and expression in a range of prostate cells

Through real-time PCR analysis, ECE-1 mRNA levels in G7 cells were shown to be significantly reduced by 35 (96 hr) and 32% (120 hr) postinfection compared to the uninfected controls (Fig. 5*a*).

In addition to analyzing ECE-1 mRNA levels, protein expression was also studied on various prostate cell lines 96 hr postinfection by Western blotting. When prostate

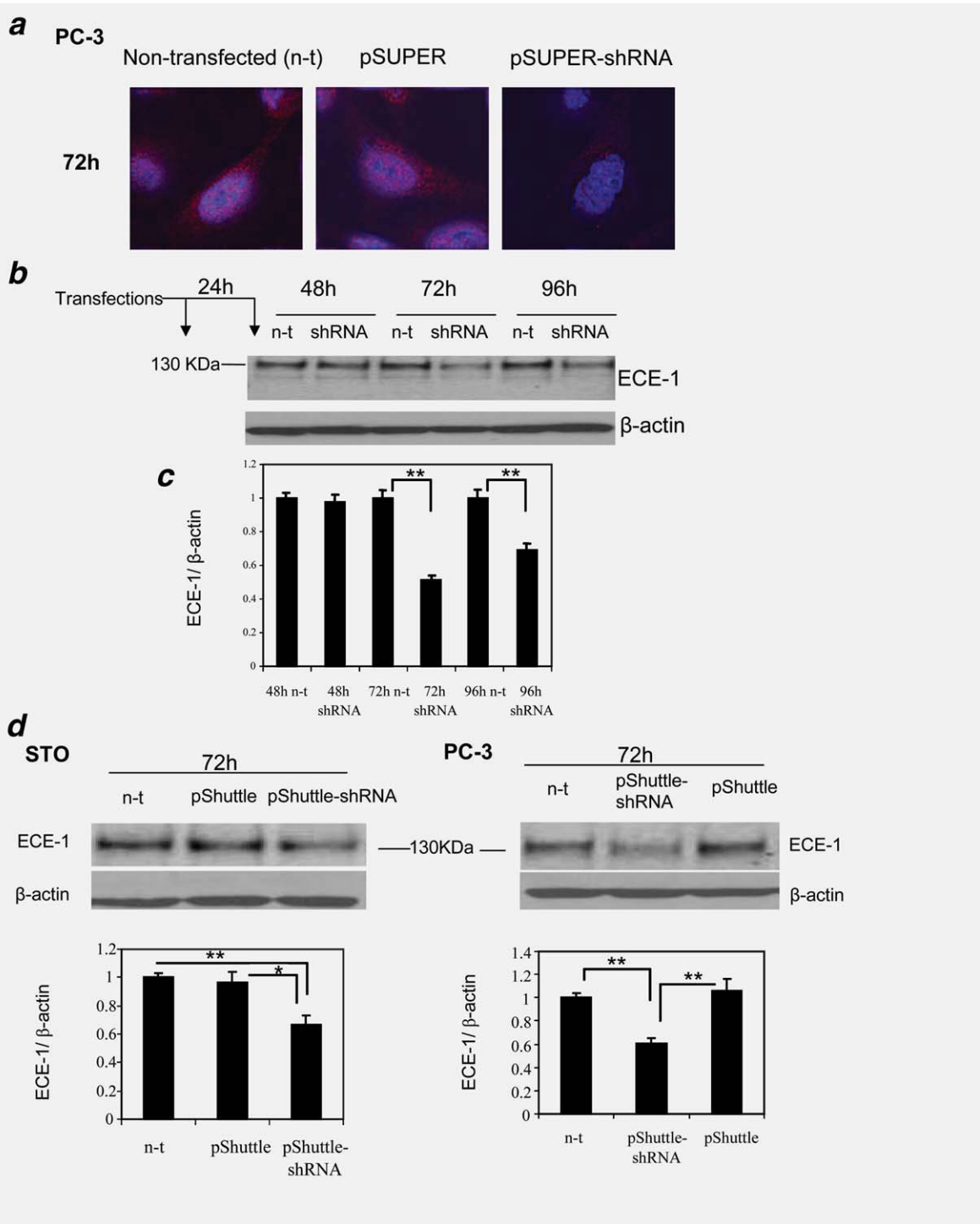

Figure 2. pSUPER/ pShuttle-link1-mediated ECE-1 shRNA reduced the levels of endogenous ECE-1 in culture cell lines. (*a*) Immunofluorescent images showing ECE-1 expression in PC-3 cells at 72 hr post-transfection. Nontransfected cells and cells transfected with pSUPER without shRNA insert were observed as a negative control. Cell nuclei stained by 1:1,000 DAPI are shown in blue, whereas ECE-1 stained by 1:20 anti-ECE-1 antibody (32–236) and Alexa Fluor 594 secondary antibody is shown in red. (*b*) Western analysis showing ECE-1 levels in PC-3 48–96 hr post-transfection. To improve transfection efficiency, a second transfection was applied 24 hr after the first. (*c*) After scanning and densitometric analysis of the ECE-1 bands detected in three independent experiments involving a "booster" transfection, relative ECE-1 levels were calculated by normalization to β-actin levels. Densities of bands were measured by Image J and presented as mean ± SD. *$p < 0.05$ and **$p < 0.001$ were considered to be statistically significant. (*d*) Western blotting showing the reduction of endogenous ECE-1 in mouse stromal cells (STO) and the human PC cell line, PC-3, transfected with pShuttle-shRNA at 72 hr. As in the case of transfection with pSUPER-shRNA, cells were transfected with pShuttle-shRNA at 0 hr and boosted with a second transfection at 24 hr. Cells transfected with "empty" pShuttle vectors and nontransfected cells were used as controls. Densitometric analysis was also carried out, and results are shown in the lower panel in (*d*). Relative ECE-1 levels were calculated by normalization to β-actin and represented as "1" in nontransfected samples.

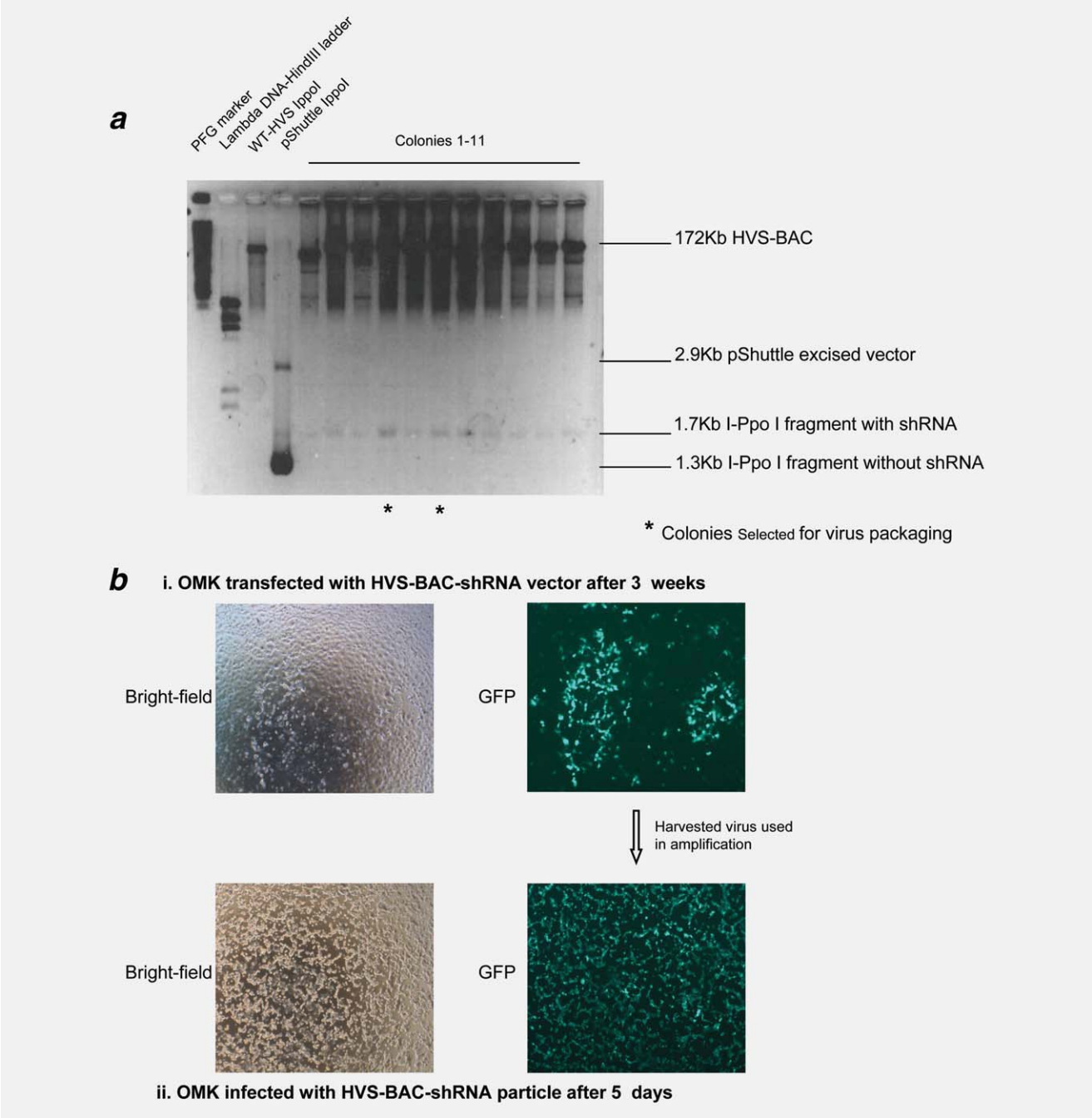

Figure 3. Construction of HVS-BAC-shRNA and packaging into virus particles. (*a*) Insert of shRNA into recombinant viral vector was checked by *I-Ppo* I digestion, followed by pulse-field gel electrophoresis (as described in Material and Methods). DNA fragments were visualized by ethidium bromide staining. (*b*) HVS-BAC-shRNA viruses were produced and amplified in the permissive OMK cells. GFP images show the virus plaques observed at week 3 post-transfection and day 5 postinfection. Bright-field images show cell density in culture wells, and GFP expression indicating infection efficiency, were observed by fluorescence microscopy at a magnification of ×4.

PNT2C2 cells were infected with HVS-BAC-shRNA virus, about 60% of the ECE-1 protein was decreased at MOI = 2, but no significant decrease observed at MOI = 1 (Fig. 5*b*). Moreover, when malignant prostate PC-3 (Fig. 5*c*) and G7 (Fig. 5*d*) cells were infected with HVS-BAC-shRNA (MOI = 2), a dramatic decrease of ECE-1 was observed in both cell types compared to their uninfected or WT-HVS-BAC controls, resulting in about 60% less ECE-1 in PC-3 and 90% less in G7 cells than the control ECE-1 levels in uninfected cells. These results indicated that HVS-based delivery of ECE-1 shRNA resulted in a much greater depletion of ECE-1 compared to a transfection-based delivery model.

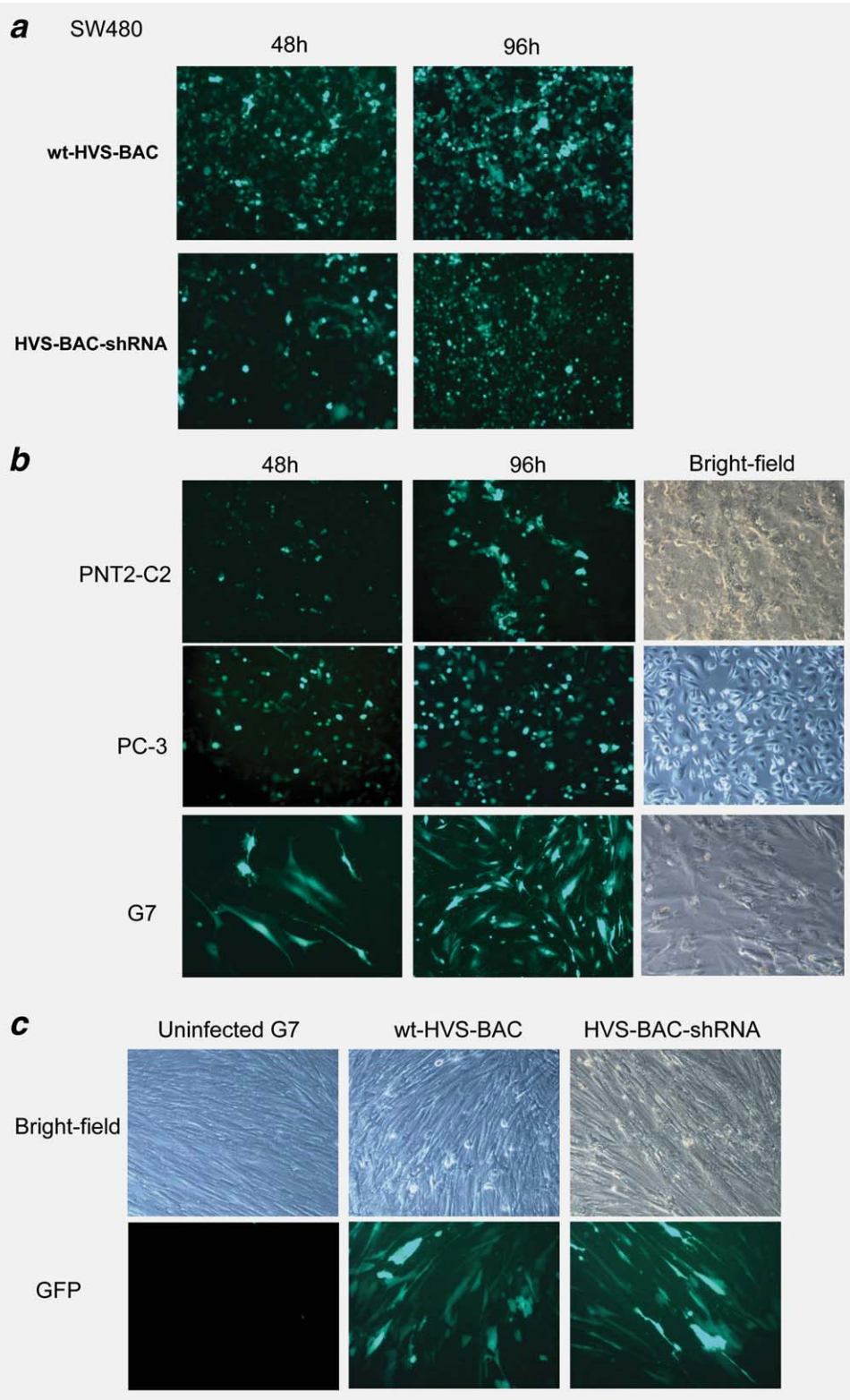

Figure 4. Infection of HVS-BAC-shRNA examined on human carcinoma cell lines. (*a*) Colorectal carcinoma cells SW480 were infected with WT-HVS-BAC and HVS-BAC-shRNA. As a recognized cell line that was previously reported to show high efficiency after HVS-BAC infection, SW480 cells were used as a positive control. (*b*) HVS-BAC-shRNA infection efficiency was tested on a range of human prostate cells: normal, transformed PNT2C2 and malignant PC-3 and G7 primary stromal cells. All infections were carried out at a MOI of 2 and observed at 48 and 96 hr postinfection by fluorescence microscopy at a magnification of $\times 10$. Cell densities were shown under bright-field conditions. (*c*) G7 cells were infected either with WT-HVS-GFP or HVS-BAC-shRNA at a MOI $= 2$ and incubated up to 120 hr. Growth of infected cells at 120 hr was monitored as bright-field image, and infection efficiency was indicated by GFP.

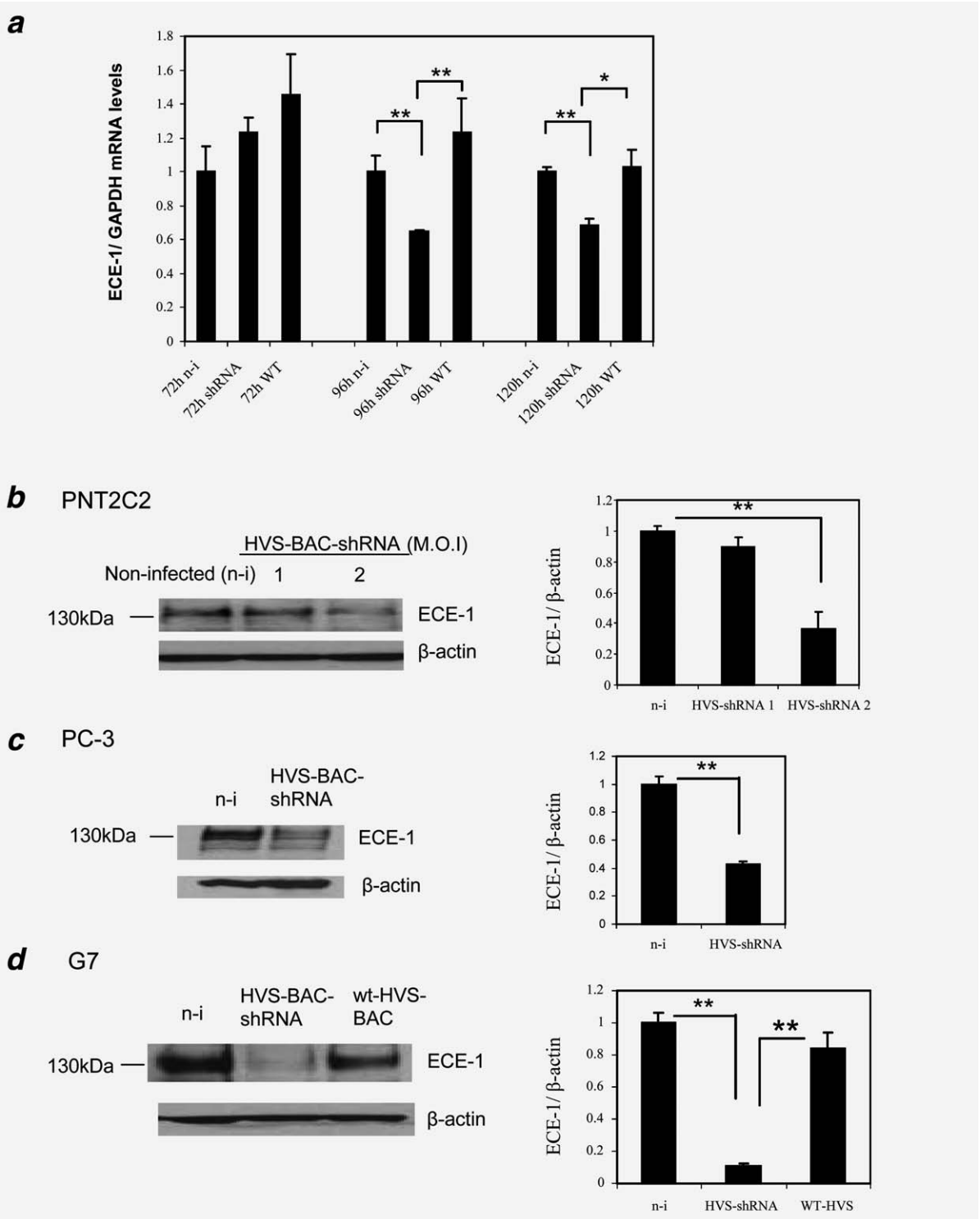

Figure 5. Viral delivery of ECE-1 shRNA reduced endogenous ECE-1 at mRNA and protein levels in infected PC cells. (*a*) Real-time PCR analysis of ECE-1 levels in HVS-BAC-shRNA-transduced G7 cells. Cells were presplit and allowed to achieve a confluency of 80–90% on the day of use. Viruses, at a MOI value of 2, were loaded directly into the cell culture medium, and the medium was replaced with fresh medium after 48 hr incubation. Cells were then harvested at 72, 96 and 120 hr postinfection for analysis. Results were achieved from three independent experiments and presented as mean ± SD. (*b*) Western blotting image showing ECE-1 knockdown in HVS-BAC-shRNA virus-infected PNT2C2. Cells were either noninfected or infected with viruses at a MOI of 1 or 2 as described in Material and Methods and harvested for analysis after 96 hr incubation. (*c*) PC-3 and (*d*) G7 cells were either noninfected or infected with HVS-BAC-shRNA at MOI = 2 and harvested for analysis after 96 hr incubation. Cells infected with WT-HVS-BAC were used as a negative control. ECE-1 proteins were detected using 1:200 anti-ECE-1 antibody (32–236) followed by ECL visualization. Beta-actin was detected as loading control. Densitometric results for each cell type are shown on the right-hand side in (*b–d*). Relative ECE-1 levels were calculated by normalization to β-actin and represented as "1" for noninfected samples. Results are presented as mean ± SD, and $*p < 0.05$ and $**p < 0.001$ are indicated in the figures to show statistical significance.

HVS-BAC-shRNA-induced ECE-1 knockdown decreased the invasive ability of PC-3 cells

Previous studies have reported that the interaction between stromal cells from prostate malignancies could enhance epithelial cell invasion in human prostate.[34] This process is thought to be mediated by an ET-1 mitogenic effect. We therefore tested whether suppression of ECE-1 could reduce invasion of PC cells. To demonstrate this, we used G7 stromal cells and epithelial PC-3 cells in a Matrigel coculture invasion model. When PC-3 cells were cocultured with HVS-BAC-shRNA-transduced G7 cells, a 33% decrease in PC-3 invasion was observed compared to non- and WT-HVS-BAC transduced G7 cells (Fig. 6*a*). Similarly, a 31% reduction in PC-3 invasion was observed in the reciprocal experiment using HVS-GFP-shRNA-transduced PC-3 cells in coculture with untreated G7 stromal cells (Fig. 6*a*). Hence, ECE-1 knockdown in either stromal cells or malignant epithelial cells does indeed suppress prostate epithelial cell invasion. Furthermore, this suppressive effect could be largely reversed by adding exogenous ET-1 (100 nM), resulting in an increase of HVS-BAC-shRNA-transduced PC-3 cell invasion from 62 to 88%, compared to the level in wt-HVS-BAC-transduced controls (Fig. 6*b*). In parallel, secretion of endogenous ET-1 was measured in HVS-BAC-shRNA-transduced PC-3 cells and found to be reduced ~30% compared to that in noninfected controls (Fig. 6*d*).

HVS-BAC-shRNA-induced ECE-1 knockdown decreased the migration rate of PC-3 cells

A scratch assay was carried out to test the cell migration rate of PC-3 cells after HVS-BAC-shRNA infection. As shown in Figure 6*c*, PC-3 cells were highly infected by both WT-HVS-BAC and HVS-BAC-shRNA (MOI = 2). During a 24-hr incubation, the scratch on the untreated cell monolayer had regrown by ~60% after 12 hr and was fully closed at 24 hr. WT-HVS-BAC-transduced PC-3 cells showed the same migration rate as untreated cells. In contrast, the width of the scratch on the HVS-BAC-shRNA-transduced PC-3 monolayer remained unchanged after 12-hr incubation and slightly reduced after 24 hr. Moreover, by adding exogenous ET-1 (100 nM) to HVS-BAC-shRNA-transduced cell cultures, cell migration could be largely recovered to a rate comparable to that in untreated cells resulting in 76% of scratch area healed within 24 hr. These observations demonstrate the inhibitory effect of the delivery of HVS-BAC-shRNA-targeting ECE-1 on PC cell migration *in vitro*.

Discussion

Elevated levels of the ECE-1 are frequently found to correlate with PC progression[18,34] and contribute to the promotion of tumor growth, proliferation and invasion.[21,34,35] As a well-recognized mitogenic peptide, ET-1 can inhibit apoptosis in renal and colon cancers,[36,37] promote cell proliferation, survival and invasion in ovarian cancer,[38,39] melanoma[40] and in lung cancer[41] and stimulate bone metastasis in breast and PCs.[42,43] In contrast to the situation *in vitro*, the local effect of ET-1 on cancer progression *in vivo* has been recently shown to be a consequence of a balance between its mitogenic activity and vasoconstrictive activity, which has found to be able to limit tumor growth by restricting blood supply.[44]

In our study, by targeting the ET axis through ECE-1 depletion, we have examined this potential approach as a novel treatment of advanced stages of PC. We have previously used siRNA duplexes (nonisoform specific) transiently to successfully target ECE-1 and modulate proliferative behavior of oral squamous carcinoma cells.[21] Independently, using ECE-1 siRNA in ovarian carcinoma cells, the suppressive effect of ECE-1 knockdown on cell invasiveness, MMP-2 activity and epithelial-to-mesenchymal transition has been demonstrated.[45] Here, we have extended our studies to achieve sustained suppression by exploiting a novel HVS-based viral delivery system to facilitate ECE-1-shRNA transfer into PC cells. HVS is a prototype gamma-2 herpesvirus, 112 kb in length, with the "gutless" potential to package ≥120 kb of heterologous DNA.[46] Deletion of the transforming genes, STP and Tip, has eliminated its oncogenic potential and prevented it from T cell transformation, which increases the biosafety of an HVS-based vector.[47,48] The use of F-factor-based BAC allows the easy and efficient cloning and modification of viral genome in *E. coli* cells.[49] HVS vectors are attractive for their ability to establish episomal latent persistence and sustained transgene expression in human carcinoma cells.[30,50] HVS can efficiently infect solid tumor xenografts and three-dimensional spheroid cultures.[51] These results suggest that HVS-based vectors may be ideal for gene therapy applications.

We have successfully cloned, characterized and purified HVS-BAC-shRNA virus and, using an MOI of 2, achieved infection efficiencies of ≥80% for G7 stromal cells *ex vivo* and PC-3 cells *in vitro*. Invasion studies using PC-3 cells in coculture with G7 stroma infected with HVS-BAC-shRNA revealed a reduction in PC-3 invasive ability of 33%. The reciprocal study using HVS-BAC-shRNA-infected PC-3 cells in coculture with untreated G7 stromal cells revealed a similar reduced PC-3 invasive ability. Our previous[35] and current studies found that addition of exogenous ET-1 reversed the suppressive effect of ECE-1 siRNA/shRNA on PC-3 cell invasion to an extent of 85–88%. Similar results were also found by Rayhman *et al.*[45] on OVCAR3 cells, showing that cell invasiveness suppressed by ECE-1 siRNA could be restored to 75% of its original level by exogenous ET-1 (80 nM). Migration studies using a scratch assay showed that PC-3 cells infected with HVS-BAC-shRNA had reduced ability to migrate across and close an artificial scratch created in the growing cell monolayer. The observed reduction in cell migration correlated with a significant, but not complete, decrease in ET-1 secretion upon HVS-BAC-shRNA infection. After addition of extracellular ET-1, it was found that the cell

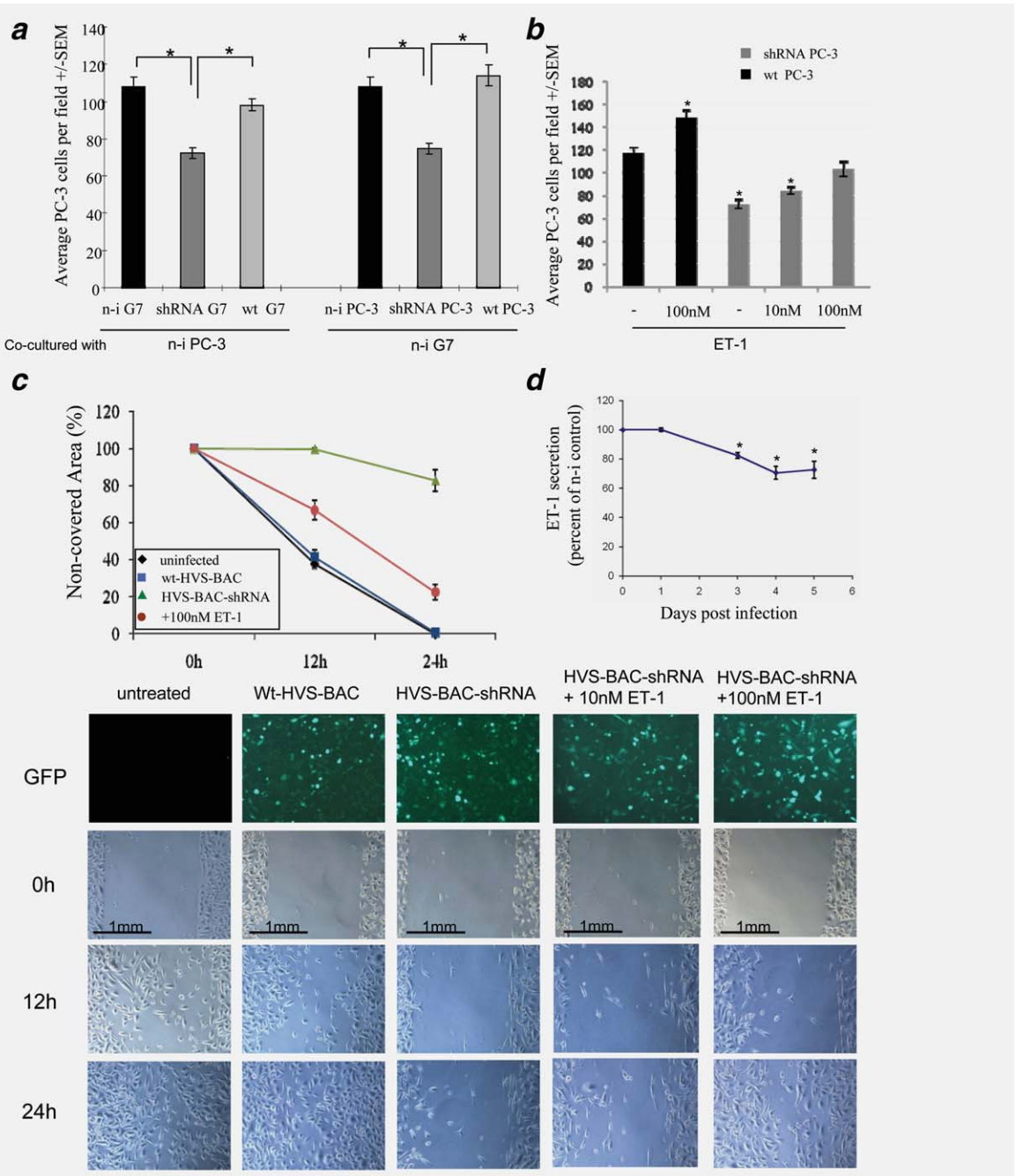

Figure 6. Influence of ECE-1 knockdown on invasiveness and migration of PC-3 cells. (*a*) Matrigel invasion assay was carried out to measure the invasiveness of PC-3 cells in the presence of stromal G7 cells. Either uninfected or infected G7 cells were harvested 96 hr postinfection and added to the lower well of a Matrigel assay chamber and allowed 24 hr to adhere. Uninfected or infected PC-3 cells were harvested and added to the top of the Matrigel at 120 hr postinfection. The invasion assay was incubated for 24 hr and performed in duplicate wells. Cell numbers of invaded PC-3 were counted from four random fields per well. Each bar represented the mean value of eight fields counted ± SEM. *$p < 0.05$ was considered to be statistically significant. (*b*) Ninety-six hours postinfection PC-3 cells were harvested and added on top of the Matrigel, coculturing with uninfected G7 for 24 hr in the absence or presence of exogenous ET-1 supplement. Cell numbers of invaded PC-3 cells were counted from four fields per well, and *$p < 0.05$ was considered to be statistically significant. (*c*) Scratch assay showing the influence of ECE-1 knockdown on migration of PC-3 cells. PC-3 cells were preseeded in six-well plate and infected by either WT-HVS-BAC or HVS-BAC-shRNA viruses as described in Material and Methods. After 72 hr infection, scratch was created by scraping the cell monolayer using a p1000 pipette tip. Cells were incubated in culture medium and kept at 37°C for 24 hr. When exogenous ET-1 was applied, 10 and 100 nM ET-1 were added to the cultures of HVS-BAC-shRNA-infected PC-3 at 0 hr. Before applying a scratch on cell monolayers, GFP expression was visualized to confirm the efficiency of each infection. Migration of PC-3 toward the scratch was observed under bright field by ×10 magnification at 0, 12 and 24 hr time points, respectively. Quantitation of the scratch assay was achieved using web-based S.CORE image analysis. Results are presented as percentage of noncovered area and shown as mean ± SD from three independent experiments. (*d*) ELISA measurements showing the ET-1 secretion in HVS-BAC-shRNA-infected PC-3 cultures. Results were presented as a percentage in comparison to the ET-1 levels in noninfected control cells. *$p < 0.05$ was considered to be statistically significant.

migration rate of HVS-BAC-shRNA-transduced PC-3 cells was partly but not completely restored to the original level in noninfected controls. Hence, the effectiveness of ECE-1 suppression may not solely reflect the ability of ECE-1 to generate ET-1. Moreover, in a study of ECE-1 inhibition in the growth of human glioblastoma cells, Berger *et al.* found that exogenous addition of ET-1 failed to counterbalance the inhibition of growth and proliferation elicited by ECE-1 inhibitors.[52] Altogether, these and other[53] findings suggest that mechanisms additional to big ET-1 activation may be involved in ECE-1 inhibition-mediated suppression of cell proliferation and migration.

In this context, the different isoforms of ECE-1 may have distinct roles. By studying the roles of ECE-1 isoforms in PC cell lines, it was demonstrated that ECE-1a and 1c have opposing effects on cell invasion.[35] Overexpression of ECE-1c was shown to promote the transformation of a low-invasive to a highly invasive cell phenotype, whereas the expression of the ECE-1a isoform suppressed invasion, suggesting the existence of an ECE-1 signaling pathway(s) independent of its catalytic activity, and the different intracellular localization of ECE-1 isoforms may additionally account for their different effects on cell invasion.

Our rationale for using ECE shRNA gene therapy for advanced PC is strengthened by a recent study using a lentiviral system to deliver an ECE-related homolog, NEP, to suppress PC growth.[54] As NEP, an ET-1-degrading enzyme, has a tumor-suppressing effect and is frequently lost in various cancers,[55,56] the effects of NEP overexpression reinforce the concept of exploitation of ECE-1 knockdown in treatment of PC although, again, the NEP effects may be mediated both by its catalytic and noncatalytic (signaling) actions.[54] Our results confirm the potential of HVS as a candidate vector for ECE siRNA gene therapy applications using PC cells and suggest that it may be have applicability in impeding the cancer cell ability to invade and migrate. An advantage of this particular vector system is that it infects both dividing and nondividing cells, without integration, eliminating both the risk of insertional gene inactivation and spontaneous host excision. In addition, its episomal existence and species incompatibility may render it a safer option as a prospective application for therapy in humans.

References

1. Jemal A, Siegel R, Ward E, Hao Y, Xu J, Thun MJ. Cancer statistics, 2009. *CA Cancer J Clin* 2009;59:225–49.
2. Kirby R, Brawer MK, Denis LJ. Prostate cancer, 3rd edn. Oxford, UK: Health Press Limited, 2001.
3. Asham E, Shanker A, Loizidou M, Fredericks S, Miller K, Boulos PB, Bumstock G, Taylor I. Increased endothelin-1 in colorectal cancer and reduction of tumor growth by ET(A) receptor antagonism. *Br J Cancer* 2001;85: 1759–63.
4. Bagnato A, Salani D, Di Castro V, Wu-Wong JR, Tecce R, Nicotra MR, Venuti A, Natali PG. Expression of endothelin 1 and endothelin-A receptor in ovarian carcinoma: evidence for an autocrine role in tumor growth. *Cancer Res* 1999;59: 720–7.
5. Smollich M, Gotte M, Yip GW, Yong ES, Kersting C, Fischgrabe J, Radke I, Kiesel L, Wulfing P. On the role of endothelin-converting enzyme-1 (ECE-1) and neprilysin in human breast cancer. *Breast Cancer Res Treat* 2007; 106:361–9.
6. Nelson JB, Chan-Tack K, Hedican SP, Magnuson SR, Opgenorth TJ, Bova GS, Simons JW. Endothelin-1 production and decreased endothelin-B receptor expression in advanced prostate cancer. *Cancer Res* 1996;56:663–8.
7. Nelson JB, Hedican SP, George DJ, Reddi AH, Piantadosi S, Eisenberger MA, Simon JW. Identification of endothelin-1 in the pathophysiology of metastatic adenocarcinoma of the prostate. *Nat Med* 1995;1:944–9.
8. Nelson JB. Endothelin inhibition: novel therapy for prostate cancer. *J Urol* 2003; 170:S65–S68.
9. Turner A, Isaac RE, Coates D. The neprilysin (NEP) family of zinc metallopeptidases: genomics and function. *Bioessays* 2001;23:261–9.
10. Schweizer A, Valdenaire O, Nelbock P, Deuschle U, Dumas Milne Edwards JB, Stumpt JG, Loffler BM. Human endothelin-converting enzyme (ECE-1): three isoforms with distinct subcellular localizations. *Biochem J* 1997; 328:871–7.
11. Valdenaire O, Lepailleur-Enouf D, Egidy G, Thouard A, Barret A, Vranckx R, Tougard C, Michel JB. A fourth isoform of endothelin-converting enzyme (ECE-1) is generated from an additional promoter molecular cloning and characterization. *Eur J Biochem* 1999;264:341–9.
12. Hunter AR, Turner AJ. Expression and localization of endothelin-converting enzyme-1 isoforms in human endothelial cells. *Exp Biol Med* 2006;231:718–22.
13. Xu D, Emoto N, Giaid A, Slaughter C, Kaw S, deWit D, Yanagisawa M. ECE-1: a membrane-bound metalloprotease that catalyzes the proteolytic activation of big endothelin-1. *Cell* 1994;78:473–85.
14. Hoang M, Turner AJ. Novel activity of endothelin-converting enzyme: hydrolysis of bradykinin. *Biochem J* 1997;327:23–6.
15. Johnson G, Stevenson T, Ahn K. Hydrolysis of peptide hormones by endothelin-converting enzyme-1. A comparison with neprilysin. *J Biol Chem* 1999;274:4053–8.
16. Padilla B, Cottrell GS, Roosterman D, Pikios S, Muller L, Steinhoff M, Bunnett NW. Endothelin-converting enzyme-1 regulates endosomal sorting of calcitonin receptor-like receptor and beta-arrestins. *J Cell Biol* 2007;179:981–97.
17. Arun B, Kilic G, Ashfaq R, Saboorian HM, Gokaslan T. Endothelin converting enzyme-1 expression in endometrial adenocarcinomas. *Cancer Invest* 2001;19: 779–82.
18. Usmani BA, Harden B, Maitland NJ, Turner AJ. Differential expression of neutral endopeptidase-24.11 (neprilysin) and endothelin-converting enzyme in human prostate cancer cell lines. *Clin Sci* 2002;103 (Suppl 48): 314S–317S.
19. Dawson LA, Maitland NJ, Berry P, Turner AJ, Usmani BA. Expression and localization of endothelin-converting enzyme-1 in human prostate cancer. *Exp Biol Med* 2006;231:1106–10.
20. Ahmed S, Thompson J, Coulson JM, Woll PJ. Studies on the expression of endothelin, its receptor subtypes, and converting enzymes in lung cancer and in human bronchial epithelium. *Am J Respir Cell Mol Biol* 2000;22:422–31.
21. Awano S, Dawson LA, Hunter AR, Turner AJ, Usmani BA. Endothelin system in oral squamous carcinoma cells: specific siRNA targeting of ECE-1 blocks cell proliferation. *Int J Can* 2006;118:1645–52.

22. Tomar RS, Matta H, Chaudhary PM. Use of adeno-associated viral vector for delivery of small interfering RNA. *Oncogene* 2003; 22:5712–15.
23. Sharma A, Tandon M, Bangari DS, Mittal SK. Adenoviral vector-based strategies for cancer therapy. *Curr Drug Ther* 2009;4: 117–38.
24. Singer O, Verma IM. Applications of lentiviral vectors for shRNA delivery and transgenesis. *Curr Gene Ther* 2008;8:483–8.
25. Amir S, Golan M, Mabjeesh NJ. Targeted knockdown of SEPT9_v1 inhibits tumor growth and angiogenesis of human prostate cancer cells concomitant with disruption of hypoxia-inducible factor-1 pathway. *Mol Cancer Res* 2010;8:643–52.
26. Tomanin R, Scarpa M. Why do we need new gene therapy viral vectors? Characteristics, limitations and future perspectives of viral vector transduction. *Curr Gene Ther* 2004;4:357–72.
27. Grimm D, Kay MA. RNAi and gene therapy: a mutual attraction. *Hematology Am Soc Hematol Educ Program* 2007: 473–81.
28. Nguyen T, Menocal EM, Harborth J, Fruehauf JH. RNAi therapeutics: an update on delivery. *Curr Opin Mol Ther* 2008;10: 158–67.
29. Griffiths RA, Boyne JR, Whitehouse A. Herpesvirus saimiri-based gene delivery vectors. *Curr Gene Ther* 2006; 6:1–15.
30. Stevenson AJ, Cooper M, Griffiths JC, Gibson PC, Whitehouse A, Jones EF. Assessment of herpesvirus saimiri as a potential human gene therapy vector. *J Med Virol* 1999;57:269–77.
31. Stevenson AJ, Frolova-Jones E, Hall KT, Kinsey SE, Markham AF, Whitehouse A. A herpesvirus saimiri-based gene therapy vector with potential for use in cancer immunotherapy. *Cancer Gene Ther* 2000;7: 1077–85.
32. Brown C, Barnes K, Turner AJ. Anti-peptide antibodies specific to rat endothelin-converting enzyme-1 isoforms reveal isoform localization and expression. *FEBS Lett* 1998;424:183–7.
33. White RE, Calderwood MA, Whitehouse A. Generation and precise modification of a herpesvirus saimiri bacterial artificial chromosome demonstrates that the terminal repeats are required for both virus production and episomal persistence. *J Gen Virol* 2003;84:3393–403.
34. Dawson LA, Maitland NJ, Turner AJ, Usmani BA. Stromal-epithelial interactions influence prostate cancer cell invasion by altering the balance of metallopeptidase expression. *Br J Cancer* 2004;90:1577–82.
35. Lambert L, Whyteside AR, Turner AJ, Usmani BA. Isoforms of endothelin-converting enzyme-1 (ECE-1) have opposing effects on prostate cancer cell invasion. *Br J Cancer* 2008;99:1114–20.
36. Eberl L, Egidy G, Pinet F, Juillerat-Jeanneret L. Endothelin receptor blockade potentiates FasL-induced apoptosis in colon carcinoma cells via the protein kinase C-pathway. *J Cardiovasc Pharmacol* 2000;36:S354–S356.
37. Pflug B, Zheng H, Udan MS, Antonio JM, Marshall FF, Brooks JD, Nelson JB. Endothelin-1 promotes cell survival in renal cell carcinoma through the ET_A receptor. *Cancer Lett* 2007;246:139–48.
38. Bagnato A, Tecce R, Moretti C, Castro V, Spergel D, Catt KJ. Autocrine actions of endothelin-1 as a growth factor in human ovarian carcinoma cells. *Clin Cancer Res* 1995;1:1059–66.
39. Rosano L, Spinella F, Di Castro V, Decandia S, Nicotra MR, Natall PG, Bagnato A. Endothelin-1 is required during epithelial to mesenchymal transition in ovarian cancer progrression. *Exp Biol Med* 2006;231:1128–31.
40. Yohn J, Smith C, Stevens T, Hoffman TA, Morelli JG, Hurt DL, Yanagisawa M, Kane MA, Zamora MR. Human melanoma cells express functional endothelin-1 receptors. *Biochem Biophys Res Commun* 1994;201: 449–57.
41. Zhang W, Zhou J, Ye QJ. Endothelin-1 enhances proliferation of lunf cancer cells by increasing intracellular free Ca^{2+}. *Life Sci* 2008;82:767–71.
42. Dreau D, Karaa A, Culberson C, Wyan H, McKillop IH, Clemens MG. Bosentan inhibits tumor vascularization and bone metastasis in an immunocompetent skin-fold model of breast carcinoma cell metastasis. *Clin Exp Metastasis* 2006;23: 41–53.
43. Van Sant C, Wang G, Anderson MG, Trask OJ, Lesniewski R, Semizarov D. Endothelin signaling in osteoblasts: global genome view and implication of the calcineurin/NFAT pathway. *Mol Cancer Ther* 2007;6:253–61.
44. Weydert CJ, Esser AK, Mejia RA, Drake JM, Barnes JM, Henry MD. Endothelin-1 inhibits prostate cancer growth in vivo through vasoconstriction of tumor-feeding arterioles. *Cancer Biol Ther* 2009;8:720–9.
45. Rayhman O, Klipper E, Muller L, Davidson B, Reich R, Meidan R. Small interfering RNA molecules targeting endothelin-converting enzyme-1 inhibit endothelin-1 synthesis and the invasive phenotype of ovarian carcinoma cells. *Cancer Res* 2008;68:9265–73.
46. Macnab S, White R, Hiscox J, Whitehouse A. Production of an infectious Herpesvirus saimiri-based episomally maintained amplicon system. *J Biotechnol* 2008;134: 287–96.
47. Duboise SM, Guo J, Czajak S. STP and Tip are essential for herpesvirus saimiri oncogenicity. *J Virol* 1998;72:1308–13.
48. Toptan T, Ensser A, Fickenscher H. Rhadinovirus vector-derived human telomerase reverse transcriptase expression in primary T cells. *Gene Ther* 2010;17: 653–61.
49. Calderwood MA, White RE, Whitehouse A. Development of herpesvirus-based episomally maintained gene delivery vectors. *Expert Opin Biol Ther* 2004;4: 493–505.
50. Griffiths R, Whithouse A. Herpesvirus saimiri episomal persistence is maintained via interaction between open reading frame 73 and the cellular chromosome-associated protein MeCP2. *J Virol* 2007;81: 4021–32.
51. Smith PG, Burchill SA, Brooke D, Coletta PL, Whitehouse A. Efficient infection and persistence of a herpesvirus saimiri-based gene delivery vector into human tumor xenografts and multicellular spheroid cultures. *Cancer Gene Ther* 2005; 12:248–56.
52. Berger Y, Dehmlow H, Blum-Kaelin D, Kitas EA, Loffler BM, Aebi JD. Endothelin-converting enzyme-1 inhibition and growth of human glioblastoma cells. *J Med Chem* 2005;48:483–98.
53. Whyteside AR, Hinsley EE, Lambert LA, McDermott PJ, Turner AJ. ECE-1 influences prostate cancer cell invasion via ET-1-mediated FAK phosphorylation and ET-1-independent mechanisms. *Can J Physiol Pharmacol* 2010; 88:850–4.
54. Horiguchi A, Zheng R, Goodman OB, Jr, Shen R, Guan H, Hersh LB, Nanus DM. Lentiviral vector neutral endopeptidase gene transfer suppresses prostate cancer tumor growth. *Cancer Gene Ther* 2007; 14:583–9.
55. Papandreou CN, Usmani B, Geng Y, Bogenrieder T, Freeman R, Wilk S, Finstad CL, Reuter VE, Powell CT, Scheinberg D, Magill C, Scher HI, et al. Neutral endopeptidase 24.11 loss in metastatic human prostate cancer contribute to androgen-independent progression. *Nat Med* 1998;4:50–7.
56. Gohring B, Holzhausen HJ, Meye A, Heynemann H, Rebmann U, Langner J, Riemann D. Endopeptidase 24.11/ CD10 is down-regulated in renal cell cancer. *Int J Mol Med* 1998;2:409–14.